NIPPON STEEL TECHNICAL REPORT No. 133 MARCH 2025

Technical Report / Research

Development of Wear Prediction Technology and Profile Optimization Technology for Railway Wheel Tread

Yosuke YAMAZAKI* Takanori KATO

Abstract

In this study, we developed a wheel wear prediction technology for railroad wheels using a 1/10-scaled wheelset roller test rig and multi-body dynamics simulation, and also developed a wheel tread profile optimization technology to generate wheel tread profiles with superior wear resistance performance based on baseline wheel tread profiles. In the wheel wear prediction technology, wheel wear is predicted using wheel wear characteristics obtained from wheelset roller rig tests, and it was shown that the wheel wear conditions of the vehicle test can be reproduced. In the wheel tread profile optimization technology, wheel specimens with optimized wheel profiles are fabricated and subjected to the wheelset roller rig test to verify the effect of optimization, and it was shown that the wheel profile has superior wear resistance compared to conventional wheel profiles.

1. Introduction

The railway vehicle wheel is worn through the repetition of the rolling contact with a rail, and the contact surface with the rail is called tread or flange, and their profiles change during service. The change in the profiles due to wear exerts a great influence on the durability, the vehicle curve negotiation performance, and derailment safety. Accordingly, it is important to evaluate the transition of the wear of a vehicle wheel under various running conditions. Furthermore, suppression of the wheel wear is important because it contributes to the enhancement of the aforementioned wheel durability, the vehicle curve negotiation performance, and derailment safety. As the evaluation method of the wheel wear, generally, vehicle tests are conducted, the cross-sectional profile of the wheel is measured periodically, and the change in the cross-sectional profile vs. travelling mileage is investigated.[1] However, this method requires a very long time and huge cost. Therefore, wear simulations predicting the cross-sectional wheel wear profile are used.[2, 3] For the wear simulation, the law of wear proposed by Lewis et al.[4] or Archard et al.[5] is often employed, and the wheel wear characteristics are crucial in these laws of wear. The wheel wear characteristics show the relationship between the wear material weight loss corresponding to the rolling contact mileage of the wheel with rails and the factors which influence the wear such as the tangential force on the contact surface, slip ratio, and the area of contact. However, since the wheel wear characteristics vary depending on the contact conditions with rails,[6] it is difficult to derive the wheel wear characteristics precisely. Therefore, in this research, we developed the wheel wear prediction technology by the combined use of the convenient, time and cost saving 1/10-scaled wheelset roller test rig and the multi-body dynamics simulation (hereafter referred to as MBD simulation) which enables the reproduction of the state of contact of a running vehicle wheel with a rail. Furthermore, on the basis of the baseline wheel tread profile, we developed the optimization technology based on the genetic algorithm[7] (hereafter referred to as GA) which generates a tread profile excellent in wear resistance. In order to verify the effect of optimization, wheel specimens having the tread profile obtained were prepared, and the evaluation of wear was performed by the wear test using a wheelset roller test rig. Such a test is hereafter referred to as the wheelset roller rig test.

2. Wear Characteristics of Wheel

In this chapter, for the purpose of obtaining the rolling distance, wear material weight loss, tangential force on the contact surface, slip ratio, and the contact surface area required for the wheel wear prediction, the method to derive wheel material wear characteristics by using the wheelset roller test rig is explained.

2.1 Overview of wear characteristics

The wear characteristics are obtained with the following procedure along the flow shown in **Fig. 1**.

* Dr. Eng., Senior Researcher, Research Section-II, Applied Mechanics Research Dept., Materials Reliability Research Lab., Steel Research Laboratories
1-8 Fuso-Cho, Amagasaki City, Hyogo Pref. 660-0891

① Conduct a wheelset roller rig test, and measure the rolling distance D and the wheel wear material weight loss M.
② Develop an MBD simulation model taking into account the contact of the wheel with the roller, and calculate the parameters (tangential force T between the wheel and the roller, slip ratio γ, contact area A) required for deriving a wear map expressing the wear characteristics.
③ Develop a wear map by using the tangential force T, slip ratio γ, and the contact area A obtained by the MBD simulation and the rolling distance D and the wear material weight loss M obtained by the wheelset roller rig test.

Details of this flow are explained hereunder.

2.2 Wheelset roller rig test

2.2.1 Test specimen

The material of the specimen conforms to the Class C wheel steel (0.7% C) specified by the Association of American Railroads Standard (hereafter referred to as the AAR Standard), and the hardness is HV 330. **Figure 2** shows an optical microscopic photograph of the microstructure of the wheel steel. This material has a fine pearlite structure. As described later, in this test, in order to simulate the state of the wheelset, two wheel specimens and two roller specimens were used. As shown in **Fig. 3**, wheel specimens were taken from the rim of a real wheel, and the roller specimens were made from the same material as the wheel by machining after quenching and tempering. **Figures 4** and **5** show the specimen dimensions and the cross-sectional profiles, respectively. The wheel specimen has the same profile as the AAR Standard wide-flange wheel,[8] with a scale ratio of 1:10. The diameter of the wheel specimen is 120 mm and its thickness is 14.5 mm. The roller specimen has the same geometry as the 136RE type rail[9] of the standard defined by the American Railway Engineering and Maintenance-of-Way Associa-

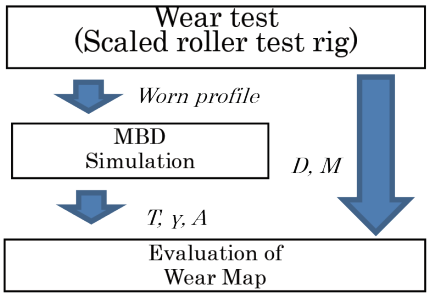

Fig. 1 Flow of deriving wear characteristics

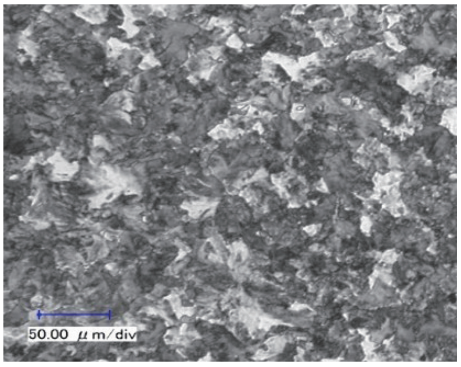

Fig. 2 Microstructure of test material

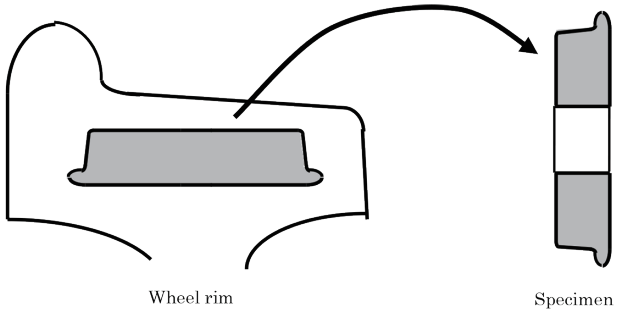

Fig. 3 Overview of wheel specimen sampling method

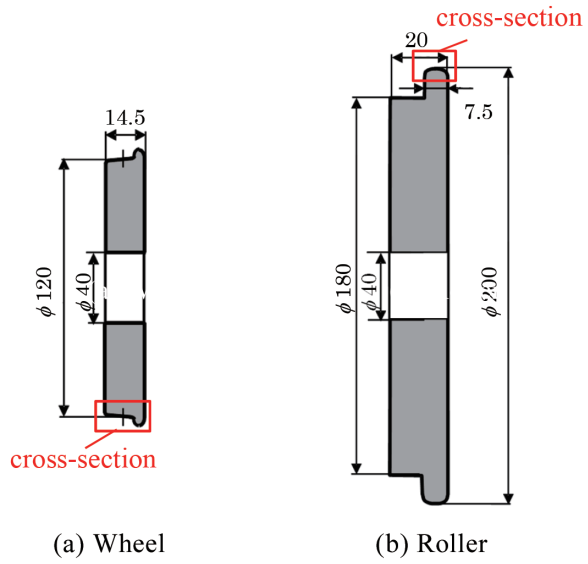

Fig. 4 Specimen dimensions

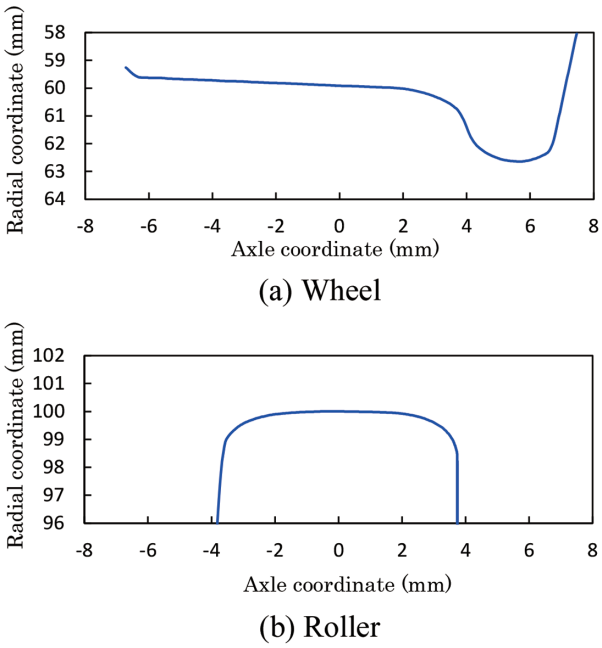

Fig. 5 Specimen cross-section profile

tion (AREMA) (hereafter referred to as the AREMA Standard) with a scale ratio of 1:10. The diameter of the roller specimen is 200 mm and its thickness is 20 mm.

2.2.2 Test condition

As shown in **Fig. 6**, the test is conducted by first bringing the two roller specimens into contact with the left and right wheel specimens respectively, and then by driving them. Next, to the axle shaft with a wheel built in on either side (hereafter referred to as the wheelset), a vertical load of 3.12 kN is exerted at its center, and a lateral load of 1.3 kN or 0.65 kN (hereafter referred to as the lateral force) is exerted. Herein, the two conditions of the lateral force were decided assuming that the vehicle runs on a small radius curved track and a medium radius curved track, respectively. Furthermore, assuming that the wheel on the upstream side of the lateral force direction contacts the rail on the outer side of a curved track, the wheel on the outer side rail is therefore termed as the outer wheel, and that the wheel on the opposite side contacts the inner side rail of the curved track, the wheel on the inner side rail is therefore termed as the inner wheel. The outer wheel contacts the outer rail at the throat section and the flange section, and the inner wheel contacts the rail only at the tread section. Herein, as **Fig. 7** shows, the contact section having a contact angle equal to or above 45 degrees is defined as the flange section, the one having a contact angle less than 3 degrees is defined as the tread section, and the section having a contact angle outside of the above is defined as the throat section as the contact section.[6] The roller specimen was rotated at 300 rpm, and the test was conducted under a dry condition. Furthermore, in this test, in order to simulate the angle of attack which takes place between the direction of the wheelset and the direction of travelling of the wheelset when a vehicle passes on a curved track section, the relative angle of the roller with respect to the wheelset is adjusted on the roller side. In this test, the per rolling distance interval of 3.75×10^3 m, the weight of the wheel specimen, and the wear profile of the wheel specimen were measured. At the time of measurement, R.P.M, displacement, load, and torque were measured for a sampling time of 1 ms. **Table 1** shows the summarized test conditions.

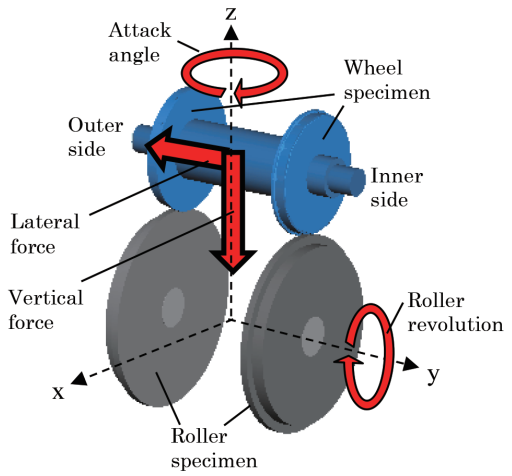

Fig. 6 Overview of wheelset roller rig test

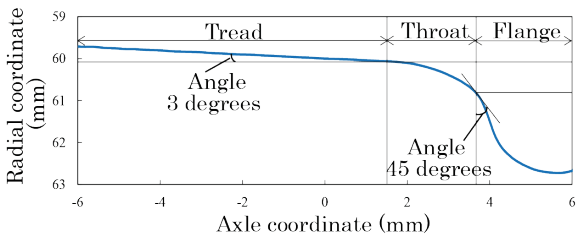

Fig. 7 Definition of wheel cross-section profile contact area

2.2.3 Rolling distance and wheel wear material weight loss

As a representative example, in **Fig. 8**, the relationship between the wear material weight loss and the rolling distance of a wheel specimen tested under the condition of Case 1 is shown, and in **Fig. 9**, the wheel cross-sectional wear profile at each rolling distance step

Table 1 Test conditions

	Revolution (rpm)		Vertical force (kN)	Lateral force (kN)	Attack angle (deg)	Lubrication
	Wheel	Roller				
Case1	500	300	3.12	1.3	0	Dry
Case2				0.65		

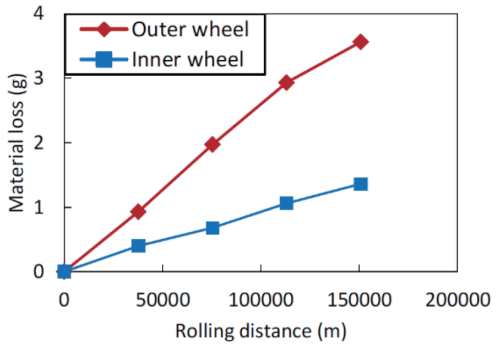

Fig. 8 Wheel material loss (Case 1)

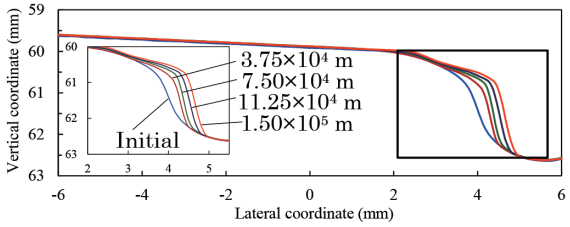

(a) Outer wheel

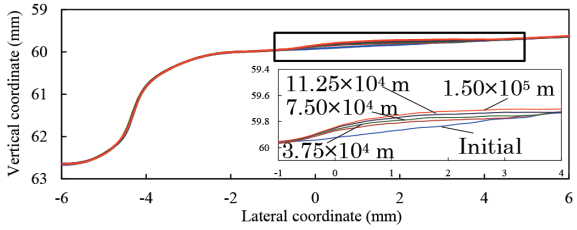

(b) Inner wheel

Fig. 9 Wheel cross-section wear profile (Case 1)

of the wheel specimen is shown. The wear material weight loss of the wheel specimen is calculated as the difference in the wheel weight between those of before and after the test. This figure shows that the wear material weight loss of the outer wheel is larger than that of the inner wheel. As above mentioned, the relationship between the rolling distance D and the wear material weight loss M was obtained for each of the two wheels of the inner wheel and the outer wheel.

2.3 MBD simulation

MBD simulation was executed using SIMPACK™ software (ver 2019) under the conditions shown in Table 1. The simulation model is a rigid body model as shown in **Fig. 10**, consisting of one wheelset and two rollers based on the specifications in **Table 2**. In the wheelset model, displacement in the front-back direction and the angle of rotation around the z axis are constrained likewise in the test machine. In the meantime, in the roller model, only the rotational angle around the y axis is allowed, and its rotational speed is set by the constraint of drive. Hertzian contact[10] is assumed at contact points of the simulation model, and for the evaluation of creep force, the FASTSIM algorithm is applied.[11] By using the cross-sectional profile obtained per the rolling distance step shown in Fig. 9, the simulation is executed, and the tangential force T, slip ratio γ, and the area of contact A at every contact point of the wheel are obtained.

2.4 Wear map

Several wear maps targeting wheels are proposed.[4, 5] In this article, among them, the wear map proposed by Lewis et al.[4] is employed. The wear map is organized by $T\gamma/A$ taken on the horizontal axis and the wear rate W on the vertical axis, and is expressed by Formula (1) below.[4]

$$W = \frac{M}{DA} = K\left(\frac{T\gamma}{A}\right) \quad (1)$$

Where, M: wear material weight loss, D: rolling distance, A: area of contact, T: tangential force, γ: slip ratio, and K: wear rate given by a function of T, γ, and A. The wear maps of the inner wheel and the outer wheel are expressed by Formulae (2), (3), and **Fig. 11** is obtained by using the tangential force T, slip ratio γ, and the area of contact A obtained by MBD simulation, and by using the rolling distance D and the wear material weight loss M obtained by the wheelset roller rig test of this time.

Outer wheel wear rate (μg/m/mm^2)

$$W = \begin{cases} 5.3\ T\gamma/A & \text{for } 0 \le T\gamma/A \le 16.55\ \text{N/mm}^2 \\ 87.72 & \text{for } T\gamma/A \ge 16.55\ \text{N/mm}^2 \end{cases} \quad (2)$$

Inner wheel wear rate (μg/m/mm^2)

$$W = \begin{cases} 5.3\ T\gamma/A & \text{for } 0 \le T\gamma/A \le 3.39\ \text{N/mm}^2 \\ 18 & \text{for } T\gamma/A \ge 3.39\ \text{N/mm}^2 \end{cases} \quad (3)$$

3. Wheel Wear Prediction

3.1 Overview of wear prediction

The wheel wear is predicted through the following procedure shown in **Fig. 12**.

① Prepare the initial wheel profile for wear prediction in the form of sequence of point.

② Develop an MBD simulation model taking into account the contact of a wheel with a rail, and obtain the output of the MBD simulation of the parameters required for the calculation of the wear of the wheel (tangential force between a wheel and a rail T, slip ratio γ, area of contact of a wheel with a rail A, and distance of travel D).

③ Calculate the wear depth by using the parameters obtained in ② above and the wear map shown in the preceding chapter.

④ Unless ③ above has reached the target running distance, reflect the updated profile in the MBD simulation, and repeat steps ②, ③, and ④ until the target distance is reached, and the wear wheel profile is finally output.

Details of this flow are explained hereunder.

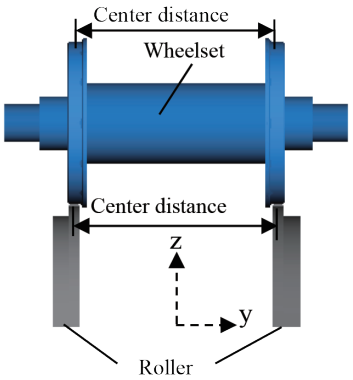

Fig. 10 Overview of MBD simulation model

Table 2 MBD simulation model conditions

Item			Value
Wheelset	Mass [kg/axle]		7.162
	Inertia moment [kg m^2]	Rolling	3.19×10^{-2}
		Pitching	6.62×10^{-3}
		Yawing	3.19×10^{-2}
	Center distance [m]		1.48
	Diameter [mm]		120
Roller	Mass [kg/specimen]		4.135
	Inertia moment [kg m^2]	Rolling	9.00×10^{-3}
		Pitching	1.78×10^{-2}
		Yawing	9.00×10^{-3}
	Center distance [m]		1.50
	Diameter [mm]		200

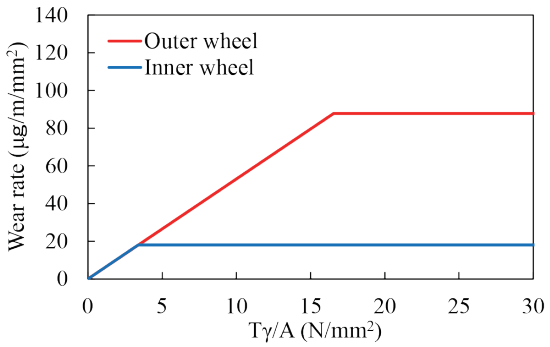

Fig. 11 Wear rate vs. $T\gamma/A$ for roller rig wear test (wear map)

3.2 MBD simulation

MBD simulation is executed by using the wheelset·roller model described in Section 2.3. The number of revolutions of the roller, vertical load, lateral load, and the angle of attack are set based on the track conditions of the vehicle test, measurement results of running speed,vertical force, and lateral force, and the information of the angle of attack obtained from the analysis of vehicle motion.

3.3 Calculation of wear depth

The wear depth is calculated as follows. The contact area of one point of a wheel on the roller is assumed to be of an elliptical shape having a major axis of a and a minor axis of b as shown in **Fig. 13**. In the area divided into a grid, the wear depth increment $\Delta Z_w(x_i, y_j)$ at the grid point (x_i, y_j) after calculation step time Δt is expressed by Formula (4) below.

$$\Delta Z_w(x_i, y_j) = K\left(\frac{T_{ij}\gamma_{ij}}{A_{ij}}\right)\frac{V\Delta t}{\rho} \quad (4)$$

Where, ρ is the density of material, V is the the wheel traveling velocity, and $K(T_{ij}\gamma_{ij}/A_{ij})$ is the wear rate given as a function of tangential force T_{ij}, slip ratio γ_{ij}, and the contact area A_{ij}.

The wear rate used in the wear prediction of this time was calculated by using the wear map obtained by the wheelset roller rig test mentioned in Section 2.2. The average wear depth in a contact area is assumed to be $\Delta\bar{Z}_w(y_j)$, which is obtained by integrating Formula (4) from $-a(y_j)$ to $a(y_j)$ along the x axis, the integrated value being divided by the peripheral length of the roller $2\pi r(y_j)$ for balancing, and expressed by Formula (5) below.

$$\Delta\bar{Z}_w(y_j) = \frac{1}{2\pi r(y_j)}\frac{V\Delta t}{\rho}\int_{-a(y_j)}^{a(y_j)} K\left(\frac{T_{ij}\gamma_{ij}}{A_{ij}}\right)dx \quad (5)$$

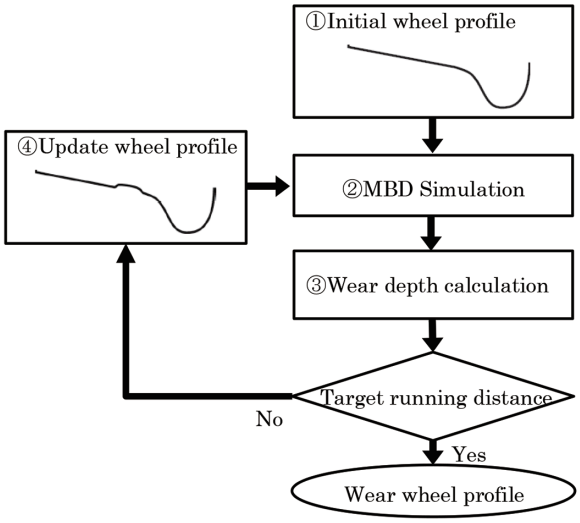

Fig. 12 Flow of wheel wear prediction

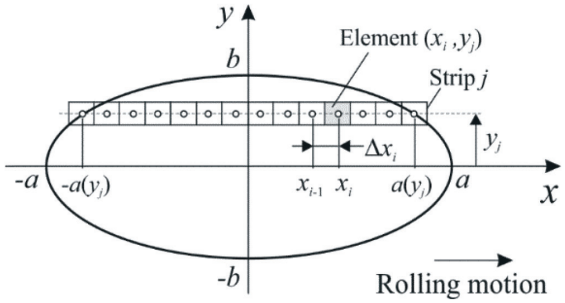

Fig. 13 Discretized contact patch

4. Reproduction of Wear Form of Real Wheel in Vehicle Test

In this chapter, reproduction of the wear form of a real wheel in the vehicle test was attempted by using the wear prediction technology explained in the preceding chapter.

4.1 Vehicle test

The vehicle test was conducted on the vehicle test track of a 4.34 km circuit called the High Ton Loop (hereafter referred to as HTL)[12] which is one of the pluralities of test tracks at the Facility for Accelerated Service Testing (hereafter referred to as FAST) owned by the Transportation Technology Center Inc. (hereafter referred to as TTCI) in Pueblo in the State of Colorado, USA. As **Fig. 14** and **Table 3**[13, 14] show, HTL consists of three curves having a curvature of 5 degrees, one curve having a curvature of 6 degrees, and the straight sections connecting the curve sections. The vehicle consists of two bogies and one car body. The vehicle conditions and the cross-sectional profiles of the wheel and the rail used in this test are shown in **Table 4** and **Fig. 15**, respectively. The wheel profile is of the wide flange type of the AAR Standard. The rail profile is of the 136RE type of the AREMA Standard. The vehicle reverses its direction of running at every 200 rounds of travelling on the track, and travels 11 000 km in total, both eastbound travelling around the circuit track and westbound travelling around the circuit track inclusively. In this test, the running speed, vertical force, lateral force, and the derailment coefficient when it runs on the track of Sections 7 and 25 are measured by using the equipment called the Truck Performance Detector (TPD).[15] In **Table 5**, an example of the measurement results of the vehicle test is shown. In addition, after the test, the wheel profile of the first wheelset in front of the vehicle was measured.

4.2 Prediction of wear

The wear prediction was performed according to the flow in Fig.

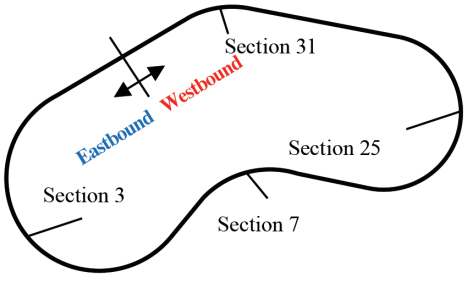

Fig. 14 Vehicle test track in TTCI (HTL)[9]

Table 3 HTL track conditions[10, 11]

Section	Curvature	Superelevation
3	5 Deg	4 inches
7	5 Deg	4 inches
25	6 Deg	5 inches
31	5 Deg	4 inches

12. Firstly, focusing on the cross-sectional profiles of the wheel and the roller shown in Fig. 5 (a) and (b), MBD simulation is executed under the conditions shown in **Table 6** decided based on the track conditions of the vehicle test shown in Table 3, the results of the measurement of the vehicle test shown in Table 5, and the angle of attack obtained from the analysis of vehicle movement mentioned in Reference[16]. Next, wear depth is calculated based on the wear map shown in Fig. 11 and Formula (4), and finally, the wheel profile is updated until it reaches 11 000 km equivalent to that in the vehicle test, and the wear profile is obtained.

4.3 Comparison of wear profiles of vehicle test with wear prediction

In **Fig. 16**, the cross-sectional wheel profiles obtained from the test vehicle and the wear prediction technology by the wheelset roller rig test are shown. These results show that the wear prediction reproduces the wear form of the real wheel in the vehicle test comparatively well, and the validity of the wear prediction technology is confirmed. With this technology, evaluation of wheel wear is possible without conducting a vehicle test.

Table 4 Vehicle conditions

Item	Value
Vehicle total weight [kg]	142 900
Distance between two bogies [m]	12.344
Wheel base [m]	1.8288
Wheel diameter [m]	0.965
Gage [m]	1.435

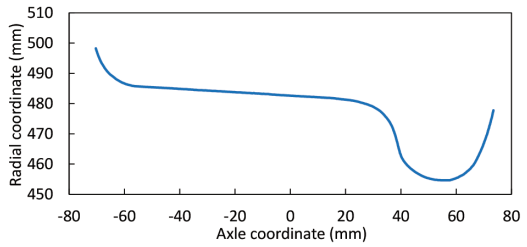

(a) Wheel

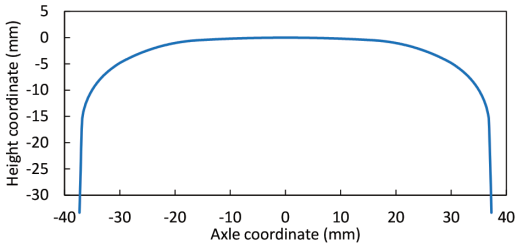

(b) Rail

Fig. 15 Cross-section profile

Table 5 Vehicle test output

	Section			
	7		25	
	Outer	Inner	Outer	Inner
Vertical force [kN]	195	165	200	160
Lateral force [kN]	35	30	72	56
Derailment coefficient [–]	0.18	0.18	0.36	0.35
Running speed [km/h]	68			

Table 6 MBD Simulation conditions

No.	Type	Time (s)	Attackangle (mrad)	Lateral load (N)	Lateral displacement (mm)
1	Straight	23	0.0	–	0.0
2	Transition curve	5	↓	↓	↓
3	Curve	9	−1.75	−550	–
4	Transition curve	3	↓	↓	↓
5	Straight	25	0.0	–	0.0
6	Transition curve	6	↓	↓	↓
7	Curve	43	−3.50	−799	–
8	Transition curve	5	↓	↓	↓
9	Straight	11	0.0	–	0.0
10	Transition curve	5	↓	↓	↓
11	Curve	16	1.75	302.0	–
12	Transition curve	5	↓	↓	↓
13	Straight	4	0.0	–	0.0
14	Transition curve	5	↓	↓	↓
15	Curve	60	−1.75	−645.0	–
16	Transition curve	3	↓	↓	↓
17	Straight	3	0.0	–	0.0

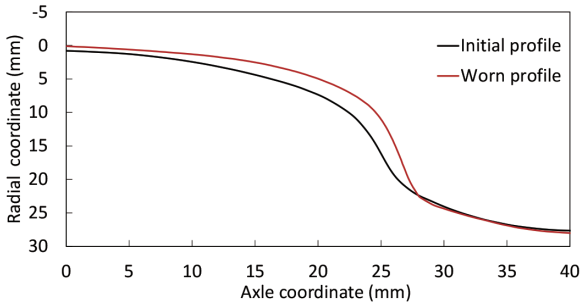

(a) Vehicle test

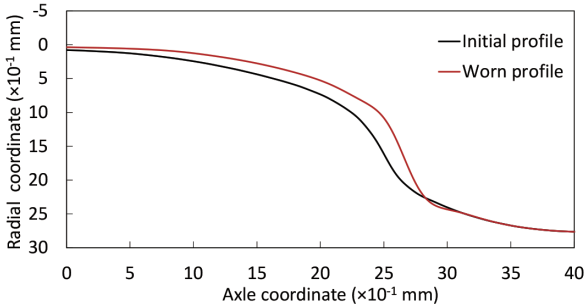

(b) Wear prediction

Fig. 16 Wear profile of wheel throat and flange area (Left side wheel)

5. Optimization of Wheel Tread Profile

5.1 Overview of optimization

Optimization of the wheel tread profile is performed in the following procedure along the flow shown in **Fig. 17**.

① Prepare the initial profile of the subject wheel in the form of the sequence of point.

② Develop an MBD simulation model taking into account the contact of the wheel with the roller, and obtain the output of the MBD simulation of the parameters required for the calculation of the wear of the wheel (tangential force between the wheel and the rail T, slip ratio γ, area of contact of the wheel with a rail A, and distance of travel D).

③ Calculate the wear depth of the wheel by using the parameters obtained in ② above and the wear map derived from the wheelset roller rig test, and calculate the wear material weight loss from the wear depth and the material density.

④ Calculate as an objective function of the minimum value of M of the wheel wear material weight loss of the revised profile (in the case of the first flow, the wheel wear material weight loss of initial profile M_0) divided by M_0 of the wheel wear material weight loss of the initial profile. When the optimization calculation reaches the target times of execution, output the updated profile as the optimized profile.

⑤ Optimize calculation based on GA to be performed by using the objective function obtained in ④ above.

⑥ Update the wheel tread profile based on the optimization calculation of ⑤ above, reflecting the latest updated profile in the MBD simulation.

5.2 Calculation of wheel wear material weight loss

The entire wheel wear material weight loss M is expressed by multiplying the wear volume produced by the difference in the wheel radius between before and after of the wear by the material density ρ, namely by Formula (6) below.

$$M = \rho\pi \sum_{j=1}^{n} \left\{ r(y_j)^2 - \left(r(y_j) - \Delta\bar{Z}_w(y_j) \right)^2 \right\} \Delta L \qquad (6)$$

Where, ΔL is the unit length of the whole width of the wheel (length in the axial direction) divided by the number of division n.

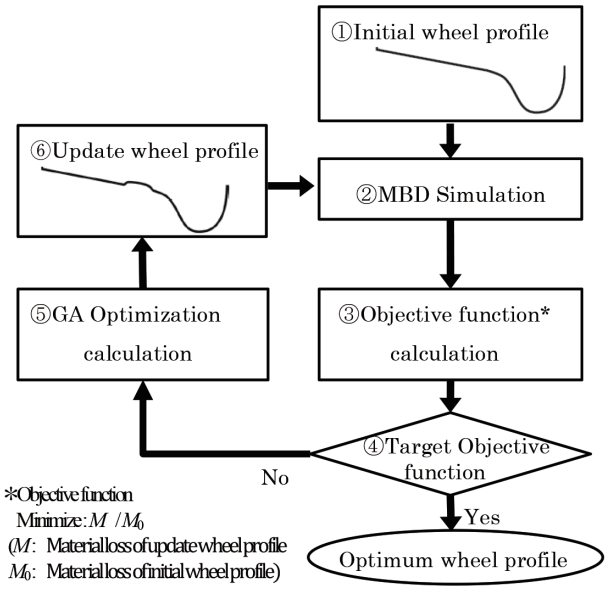

Fig. 17 Flow of wheel tread profile optimization

5.3 Optimization calculation based on GA

GA is a search method based on the biological evolution (selection, crossover, mutation, etc.),[7] which generates many candidate solutions (individuals) to a target optimization problem and applies various genetic operations to the population of candidate solutions (population set). By repeating this operation, an individual with a highly adaptive objective function is selected and the optimal solution is obtained.

Optimization of the wheel profile is performed in the three steps shown in **Fig. 18**. First, the existing wheel curvature change point is used as the design variable. Next, by using GA based on the objective function under certain restricting conditions, the design variables are moved in the radial direction. Finally, by spline-interpolating the sequence of point of data in the optimization range, the final profile is obtained.

5.4 Result of wheel profile optimization calculation

A wheelset roller rig test shown in Section 2.2 was conducted on the wheel having the optimized profile obtained from the optimization calculation of this time under the condition of Case 1 of Table 1. The worn optimized profile is shown in **Fig. 19** together with the baseline profile. The optimized profile has, shown as the initial profile in (b) of the figure, a convex portion in the throat section. The outer wheel wear material weight losses of the baseline profile and the optimized profile both sought by simulation are shown in **Fig. 20**. With this figure, it is confirmed that the wear material weight loss of the optimized profile is smaller than that of the baseline profile. The reason for wear material weight loss being smaller is due to the characteristics of the optimized profile shown earlier. With the setting of a convex portion in the throat section, lateral load is re-

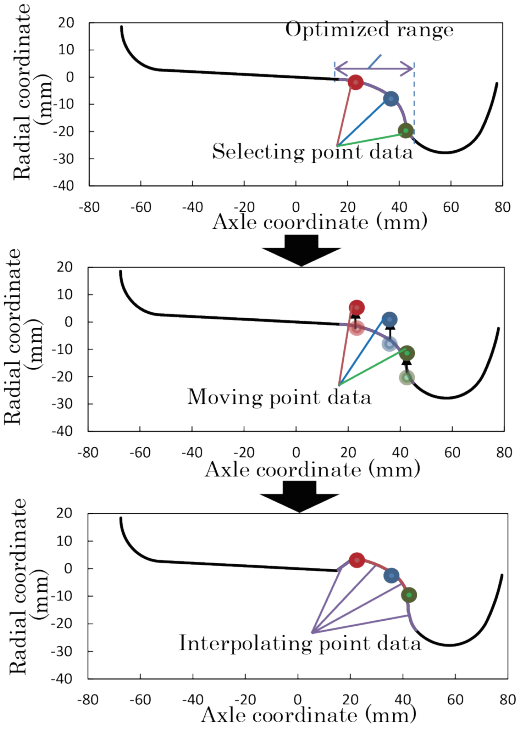

Fig. 18 Optimization procedure for wheel cross-section profile

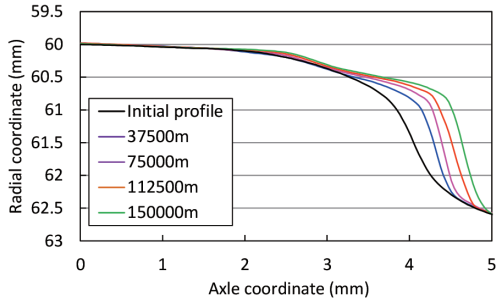

(a) Baseline profile

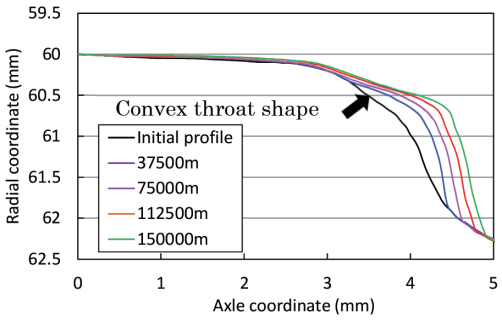

(b) Optimized profile

Fig. 19 Wheel cross-section wear profile

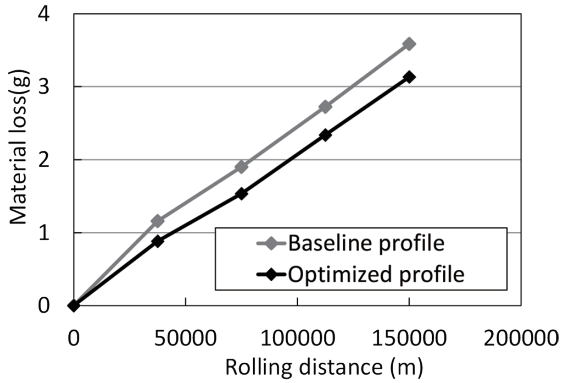

Fig. 20 Comparison of material loss between baseline and optimized profile

ceived by the two parts of the flange section and the throat section, and the load is dispersed thereby. As stated above, the wheel with the optimized profile has wear-resistance characteristics superior to that of the wheel with the baseline profile, and the validity of the optimizing technology has been confirmed. This technology is applicable to the development of long-life wheels.

6. Conclusion

This article described the development of the wheel wear prediction technology using in a combined manner the 1/10-scaled wheelset roller test rig and the multi-body dynamics simulation, and the development of the optimizing technology which generates the wheel tread profile excellent in wear-resistance characteristics based on the baseline wheel tread profile.

In the wheel wear prediction technology, firstly, we proposed the method of deriving the wheel wear characteristics by using the wheelset roller test rig, and the wear characteristics at the contact in the tread section and the contact in the throat·flange section focusing on the AAR Standard wheel were obtained. Next, we developed the wear prediction technology which estimates the wheel wear profile based on the wear characteristics obtained as above from the wheelset roller rig test and the information obtained in a vehicle test. Furthermore, we performed the wheel wear prediction for the vehicle equipped with the AAR Standard wheel which actually travelled for the test on the TTCI test track. As a result, we confirmed that the wheel wear profile of the vehicle test and the predicted wheel wear profile showed good agreement with each other.

In the wheel tread profile optimization technology, firstly, we developed the wheel tread profile optimization technology based on the genetic algorithm subject to the wheelset roller rig test. Furthermore, we performed the profile optimization for AAR Standard wheels, conducted the wear test of the wheel with the obtained optimized profile and the wheel with the baseline profile by the wheelset roller test rig, and as a result of comparing the wheel wear profiles, the wheel with the optimized profile is superior to the wheel with the baseline profile in wear-resistance characteristics, and we confirmed the validity of the optimization technology.

The railway wheel wear prediction technology developed this time enables the evaluation of the wheel wear without conducting the vehicle test. Furthermore, the wheel tread profile optimization technology is applicable to the development of long-life wheels. Hereafter, we are determined to utilize these technologies for the design and development of railway wheels.

Acknowledgements

We would like to thank Professor Hiroyuki Sugiyama (The University of Iowa), and Researcher Hiroki Yamashita (The University of Iowa) for their extensive and valuable contributions to this joint research and development project with Nippon Steel Corporation. We thank Mr. Takahiro Fujimoto (Nippon Steel Railway Technology Co., Ltd.) and Mr. Osamu Kondo (Nippon Steel Technology Co., Ltd.) for their many suggestions on this research and development.

References

1) Shi, H., Wang, J., Wu, P., Song, C., Teng, W.: Field measurements of the evolution of wheel and vehicle dynamics for high-speed trains. Vehicle System Dynamics. 56 (8), 1187–1206 (2018)
2) Pearce, T.G., Sherratt, N.D.: Prediction of Wheel Profile Wear. Wear. 144, 343–351 (1991)
3) Braghin, F., Lewis, R., Dwyer-Joyce, R., Bruni, S.: A Mathematical Model to Predict Railway Wheel Profile Evolution due to Wear. Wear. 261, 1253–1264 (2006)
4) Lewis, R., Dwyer-Joyce, R.: Wear mechanisms and transitions in railway wheel steels. Proc IMechE, PartJ: J Engineering Tribology. 218, 467–478 (2004)
5) Archard, J.F.: Contact and rubbing of flat surfaces. J Appl Phys. 24, 981–988 (1953)
6) Yamazaki, Y., Kato, T., Fujimoto, T., Kondo, O., Feldmeier, C., Sugiyama, H.: Evaluating of Wheel Wear Property with Scaled Roller Test Rig. Proceedings of the 11th International Conference on Contact Mechanics and Wear of Rail/Wheel Systems, Delft, The Netherlands, 2018, p.1156–1161
7) Kawamo, K., Yokoyama, M., Hasegawa, H.: Foundation and Application of Optimization Theory—Focused on GA and MOD—, CORONA PUBLISHING CO.,LTD.
8) Leary, J.: Final report on the development of an alternative AAR interchange wheel profile. Report no.R-706, Association of American Railroads, 1988
9) AREMA Manual, Chapter. 4—Rail, 2007 Edition
10) Kalker, J.J.: Wheel-rail rolling contact theory. Wear. 144, 1991

11) Kalker, J.J.: A fast algorithm for the simplified theory of rolling contact. Veh Syst Dyn. 11, 1–13 (1982)
12) Li, D.: 25 years of heavy axle load railway subgrade research at the Facility for Accelerated Service (FAST). Transportation Geotechnics, 2018, 17, p.51–60
13) Jimenez, R., Davis, D., Trevizo, C., Singh, S.: Crosstie and Fastener Tests at FAST: 1988–1999. AAR Reserch Report. R-937, 2000
14) Ahmadian, M.: An experimental evaluation of the effect of rail vehicles truck suspensions on wheel-rail forces. Proceedings of the 1999 ASME/IEEE Joint Railroad Conference, Dallas, TX, p.144–150
15) Singh, S.P.: Effectiveness of Wayside Detector Technologies on Train Operation Safety. United States, Department of Transportation, Federal Railroad Administration, Office of Railroad Policy and Development, No. DOT/FRA/ORD-22/19. 2022
16) Yamazaki, Y., Kato, T., Yamashita, H., Sugiyama, H., Fujimoto, T., Kondo, O.: Evaluating Wheel Wear with Scaled Roller Test Rig Considering On-Track Vehicle Test Scenarios. Proceedings of the 20th International Wheelset Congress, Chicago, USA, 2023

Yosuke YAMAZAKI
Dr. Eng., Senior Researcher
Research Section-II, Applied Mechanics Research Dept.
Materials Reliability Research Lab.
Steel Research Laboratories
1-8 Fuso-Cho, Amagasaki City, Hyogo Pref. 660-0891

Takanori KATO
Dr. Eng., Chief Manager, Head of Dept.
Railway, Automotive & Machinery Parts Research Dept.
Kansai R & D Lab.